Pharm Res (2010) 27:2374–2383
DOI 10.1007/s11095-010-0243-2

RESEARCH PAPER

Crystallization of Trehalose in Frozen Solutions and its Phase Behavior during Drying

Prakash Sundaramurthi • Thomas W. Patapoff • Raj Suryanarayanan

Received: 15 April 2010 / Accepted: 10 August 2010 / Published online: 2 September 2010

ABSTRACT

Purpose (i) To study the crystallization of trehalose in frozen solutions and (ii) to understand the phase transitions during the entire freeze-drying cycle.

Method Aqueous trehalose solution was cooled to −40°C in a custom-designed sample holder. The frozen solution was warmed to −18°C and annealed, and then dried in the sample chamber of the diffractometer. XRD patterns were continuously collected during cooling, annealing and drying.

Results After cooling, hexagonal ice was the only crystalline phase observed. However, upon annealing, crystallization of trehalose dihydrate was evident. Seeding the frozen solution accelerated the solute crystallization. Thus, phase separation of the lyoprotectant was observed in frozen solutions. During drying, dehydration of trehalose dihydrate yielded a substantially amorphous anhydrous trehalose.

Conclusions Crystallization of trehalose, as trehalose dihydrate, was observed in frozen solutions. The dehydration of the crystalline trehalose dihydrate to substantially amorphous anhydrate occurred during drying. Therefore, analyzing the final lyophile will not reveal crystallization of the lyoprotectant during freeze-drying. The lyoprotectant crystallization can only become evident by continuous monitoring of the system during the entire freeze-drying cycle. In light of the phase separation of trehalose in frozen solutions, its ability to serve as a lyoprotectant warrants further investigation.

KEY WORDS *in situ* freeze-drying XRD · lyoprotectant crystallization · phase transformation · trehalose

INTRODUCTION

Freeze-drying, also known as lyophilization, is a widely used process to dry macromolecules, diagnostic agents and other thermolabile pharmaceuticals (1). However, the stresses encountered during freeze-drying can denature proteins. Lyoprotectants can stabilize these macromolecules, both during freeze-drying and subsequent storage (2–4). This is brought about by the direct interaction of the amorphous lyoprotectant with the protein. Phase separation or crystallization of lyoprotectant, either during the freeze-drying process or subsequent product storage can adversely affect the protein stability (5–8). Non-reducing sugars, such as sucrose and trehalose, in light of their ability to remain amorphous, are widely used as lyoprotectants (1,4,9–13).

Trehalose is a naturally occurring disaccharide consisting of two α-glucose units. Due to its exceptional physical and chemical stability, trehalose is a popular lyoprotectant. In contrast to other disaccharides, amorphous trehalose is characterized by a high glass transition temperature (~117°C) (14,15). Unlike sucrose, the glycosidic linkage in trehalose is resistant to hydrolysis (16). However, the aqueous solubility of trehalose is significantly lower than that of sucrose at temperatures <60°C (17,18). Hence, at subambient temperatures employed during freeze-drying, the degree of supersaturation in trehalose solutions is much higher than in sucrose systems.

P. Sundaramurthi · R. Suryanarayanan (✉)
Department of Pharmaceutics, College of Pharmacy
University of Minnesota
Minneapolis, Minnesota 55455, USA
e-mail: surya001@umn.edu

P. Sundaramurthi
Scientific Affairs, Teva Parenteral Medicines Inc.
11 Hughes
Irvine, California 92818, USA

T. W. Patapoff
Early Stage Pharmaceutical Research and Development
Genentech, Inc.
South San Francisco, California 94080, USA

The eutectic temperature of the trehalose-water binary system, extrapolated from the solubility studies of trehalose as a function of temperature, ranges from −2.5 to −18.8°C (18–20). Such extrapolations were necessary since the high viscosity of concentrated trehalose solutions inhibited its crystallization. For example, the viscosity of ~73% w/w aqueous trehalose solution was reported to be 680 Pa·s at −23°C (18). Interestingly, there was a dramatic decrease in viscosity to 192 Pa·s when the temperature was increased to −15°C, reflecting the highly fragile nature of the trehalose freeze-concentrate. Such a pronounced temperature-dependence of viscosity was observed at temperatures higher than the glass transition temperature of the freeze-concentrate (Tg'). Based on several studies, the Tg' of trehalose is in the vicinity of −32 to −40°C. Our preliminary investigations revealed that annealing at temperatures > Tg' caused trehalose crystallization (21). The observed crystallization of trehalose was interesting in light of the numerous reports documenting amorphous trehalose in the lyophiles (2,9–11,22). It is the conventional practice to characterize the physical state of lyoprotectant by subjecting the dried product to powder X-ray diffractometry. If the lyoprotectant is amorphous in the lyophile, it is assumed that it effectively resisted crystallization in the frozen state and during drying. This assumption is not unreasonable, since a crystalline compound will not spontaneously transform into its amorphous counterpart. However, there are several examples of drying-induced transformation of a crystalline hydrate to an amorphous anhydrate. In these systems, the physical state of the product phase is often governed by the kinetics of water removal (23,24).

In our preliminary studies, we observed crystallization of trehalose as trehalose dihydrate in frozen solutions (21). These results strongly suggest the possibility of lyoprotectant phase-separation in frozen solution. We therefore hypothesize that the existence of trehalose in a substantially amorphous state in the final lyophile does not guarantee the same physical state during all the stages of freeze-drying. Trehalose crystallization in the frozen solution can be followed by a crystalline hydrate → amorphous anhydrate transition during drying. Such a processing-induced transformation, wherein there is phase separation (brought about by crystallization) in the frozen state, can still yield an amorphous final product. Once the lyoprotectant crystallizes, the phase separation can seriously impair its ability to function as a lyoprotectant in spite of its amorphous nature (5,8). The instability can be brought about by the reduction or absence of an effective interaction between protein and lyoprotectant molecules in the dried state (25).

The overall goal of this work was to understand the crystallization propensity of trehalose in frozen solutions and to continuously monitor the system during drying. Trehalose crystallization was investigated by differential scanning calorimetry and low-temperature X-ray powder diffractometry (XRD) using both laboratory and synchrotron sources. By freeze-drying trehalose solutions in the sample chamber of an X-ray diffractometer, characterization during all the stages of the freeze-drying cycle was possible. In order to determine the effect of a crystallizing solute, these studies were also conducted in a buffered (succinate) system, wherein the buffer components are known to crystallize readily (26,27). Finally, the effect of external seeding was also evaluated.

MATERIALS AND METHODS

Materials

Trehalose dihydrate and succinic acid were purchased from Sigma (>99%) and were used without further purification. All solutions were prepared with deionized water. Prior to the solution preparation, the deionized water was degassed by holding at 70°C for 5 min and filtered through 0.45 μm PTFE membrane filter (28). The degassed water, stored in a closed container at RT, was used to prepare the solutions. A pH meter (Oakton), calibrated with standard buffer solutions (Oakton standard buffers, pH 2.00, 4.01, 7.00 and 10.00, certified by NIST) was used.

Buffer solutions were prepared by dissolving the appropriate amount of succinic acid and adjusting the pH with 2 M NaOH to 4.0, 5.0 or 6.0 (±0.1) at 25°C. Appropriate amount of either trehalose or mannitol was then dissolved in the buffer solutions. All the solutions were filtered (0.45 μm PTFE, Fisher, USA) and stored in tightly closed glass vials at RT.

Lyophilization

Succinate buffer solutions of 10 mM concentration at different pH values (4.0–6.0) were prepared with either (0.5%–2% w/v) crystallizing (mannitol) or a non-crystallizing (trehalose) solute. Five milliliters of the pre-lyophilization solution was filled into glass vials and then loaded into a bench-top (VirTis® AdVantage™, Gardiner, NY) freeze-dryer. USP Type I borosilicate glass vials, (VWR®) with 20 mm neck size and 10 ml fill volume capacity were used. The freeze-dryer shelf was cooled to −50°C at 0.5°C/min, held for 1.5 h, then heated to −20°C and held for 4 h. Following this annealing step, primary drying (at 60 mTorr) was carried out at a shelf temperature of −30°C for 30 h. Secondary drying was conducted, first at −10°C for 3 h and then at +10°C for 5 h. At the end of the cycle, the vials were capped with rubber stoppers (two-

leg gray butyl, Fisher Scientific) under vacuum (at 60 mTorr) and then stored at RT.

Temperature and pH Measurement during Freezing

The buffer solution (25 ml) was placed in a jacketed beaker (100 ml) connected to a water bath with an external controller unit (Neslab RTE 740, Thermo electron, NH). A bath fluid (Dynalene® HC-50, Dynalene Heat Transfer Fluids, PA) with a working temperature in the range of 80 to −40°C was used. A low temperature pH electrode (Inlab®cool, Mettler Toledo, Switzerland) was placed in the center of the sample and connected to a pH meter (pH 500 series, Oakton, Singapore) to monitor the electromotive force (EMF). The measured EMF was then used to calculate the pH of the solution. The reference electrolyte containing glycerol and formaldehyde (Friscolyte-B™, Mettler Toledo, Switzerland) allowed the pH measurements down to −30°C. A copper-constantan thermocouple (0.05 in. diameter, Omega, Stanford, CT) with Teflon insulation connected to a digital bench-top readout device (±0.2°C; Omega MDSi8 Series, Stanford, CT) was used to monitor the temperature changes in the sample upon cooling. In all the experiments, the thermocouple was placed in the middle of the sample close to the electrode bulb.

The solutions were initially allowed to equilibrate at 0°C and then cooled to −25 at 0.5°C/min, simulating the cooling conditions in the lyophilizer. Both the temperature and pH of the solution were monitored throughout the experiment.

X-ray Diffractometry (XRD)

A powder X-ray diffractometer (Model XDS 2000, Scintag; Bragg-Brentano focusing geometry) with a variable temperature stage (High-Tran Cooling System, Micristar, Model 828D, R.G. Hansen & Associates; working temperature range: −190 to 300°C) and a solid-state detector was utilized for all low-temperature XRD studies.

About 1 mL of the aqueous solution was placed into a custom-designed sample holder and sealed with a stainless steel dome with a beryllium window. This sample holder was designed to accommodate large volumes in order to enhance the sensitivity of the instrument. Typically, the solutions were cooled from RT to −40 at 1°C/min, held for 10 min, and then heated at 1°C/min to the annealing temperature of −18°C. The annealing temperature was selected based on the thermal events reported. The eutectic melting and glass transition temperature of trehalose/water binary systems respectively were −2.5 and −35°C. During annealing, some of the samples were seeded either with trehalose dihydrate or succinic acid to induce crystallization. Another set of experiments was performed without any seeding. While the primary drying was conducted at −25°C under reduced pressure (150 mTorr), the secondary drying temperature ranged between 0 and 10°C.

The frozen mass was periodically exposed to Cu Kα radiation (45 kV×40 mA) in the reflection mode, and the XRD patterns were obtained using solid-state detector. The samples were scanned over an angular range of 5 to 40° 2θ with a step size of 0.05° and a dwell time of 1 s. The results were compared with the data in the Powder Diffraction Files (PDF) of the International Centre for Diffraction Data (ICDD) (29).

In an effort to enhance sensitivity, selected experiments were performed in the synchrotron beamline of the Midwest Universities Collaborative Team's—Sector 6, at the Advanced Photon Source, Argonne National Laboratory (Lemont, IL, USA). Details of the instrument set-up, fabrication of the sample holder to perform the studies in the transmission mode, experimental conditions, and date refinement are provided elsewhere (30).

Differential Scanning Calorimetry

A differential scanning calorimeter (MDSC, Model 2920, TA instruments, New Castle, DE) equipped with a refrigerated cooling accessory was used. Approximately 40–50 mg of aqueous trehalose solution was weighed in an open aluminum pan and cooled from RT to −70°C. Dry nitrogen, at 50 ml/min, was used as the purge gas. The frozen solution was seeded either with trehalose dihydrate or succinic acid. The seed crystals were sprinkled on the surface of the frozen solution. After seeding, the frozen solutions were warmed to −18°C and annealed for 48 h. The annealed samples were then cooled back to −50°C and rewarmed to RT. The heating and cooling rate was 1°C/min.

RESULTS AND DISCUSSION

Baseline Characterization of the Crystalline Phases

Trehalose dihydrate was characterized by DSC, XRD and thermogravimetric analysis (TGA). The diagnostic XRD peaks enabled the identification of trehalose dihydrate, α-trehalose anhydrate, succinic acid, monosodium succinate and disodium succinate. Trehalose dihydrate was characterized by peaks (Cu Kα radiation; λ=1.5407 Å) at 8.8° (10.10 Å), 12.6° (7.00 Å), 13.7° (6.45 Å), and 16.5° 2θ (5.36 Å) while the anhydrate was identified by the peaks at 16.8° (5.26 Å) and 17.8° 2θ (4.98 Å). The unique peaks of β-succinic acid [20.1° (4.41 Å) and 26.0° 2θ (3.42 Å)], monosodium succinate [14.0° (6.32 Å) and 17.8° 2θ (4.98

Å)], and disodium succinate [11.9° 2θ (7.43Å)] facilitated physical characterization of multiple phases in a single system.

Characterization of the Final Lyophile

We had observed crystalline trehalose in the final lyophile for the first time, when a trehalose solution buffered with succinic acid was freeze-dried (21). In order to understand the crystallization behavior of trehalose, it was therefore instructive to first characterize the final lyophiles. When succinic acid, buffered in the pH range of 4 to 6 was freeze-dried, the final lyophile contained crystalline buffer components (27). The XRD images of the lyophiles prepared from solutions buffered to pH values of 4.0 (panels 1–3) and 6.0 (panels 4–6) are given in Fig. 1. As discussed earlier, the Debye rings in panel 1 were attributed to succinic acid and monosodium succinate, while those in panel 4 to monosodium and disodium succinate (26). Trehalose, which is widely believed to be a non-crystallizing solute, was added in an effort to inhibit buffer crystallization. As is evident from Fig. 1, trehalose appeared to *facilitate* crystallization of buffer components at pH 4.0 (panel 2), while it inhibited crystallization at pH 6.0 (panel 5). In order to facilitate visualization, a section of panel 2 was expanded, and some characteristic Debye rings of succinic acid, monosodium succinate and trehalose dihydrate were labeled (Fig. 2). While some of the peaks were not attributable to any of the buffer components, their positions matched with that of trehalose dihydrate (Fig. 2). When a buffer solution was lyophilized with mannitol, a readily crystallizing solute, buffer crystallization was readily evident at both pH values (panels 3 and 6, Fig. 1). Thus mannitol appeared to facilitate buffer component crystallization.

The effect of trehalose and mannitol on the crystallization of monosodium succinate can be gauged from Fig. 3. Only at pH 4.0, the influence of mannitol was very pronounced. The pronounced crystallization of monosodium succinate in the presence of trehalose (evident when compared with the control) was very surprising. In light of the inability of trehalose to inhibit buffer crystallization, we hypothesized that the crystallized buffer components in the frozen solution facilitated trehalose dihydrate crystallization, which in turn facilitated further crystallization of buffer components. The following experiments were conducted to test this hypothesis: (i) low-temperature pH measurement of the buffer solution containing trehalose, (ii) low-temperature XRD (both laboratory and synchrotron) and DSC of frozen trehalose solution, (iii) freeze-drying of trehalose solution in the X-ray diffractometer.

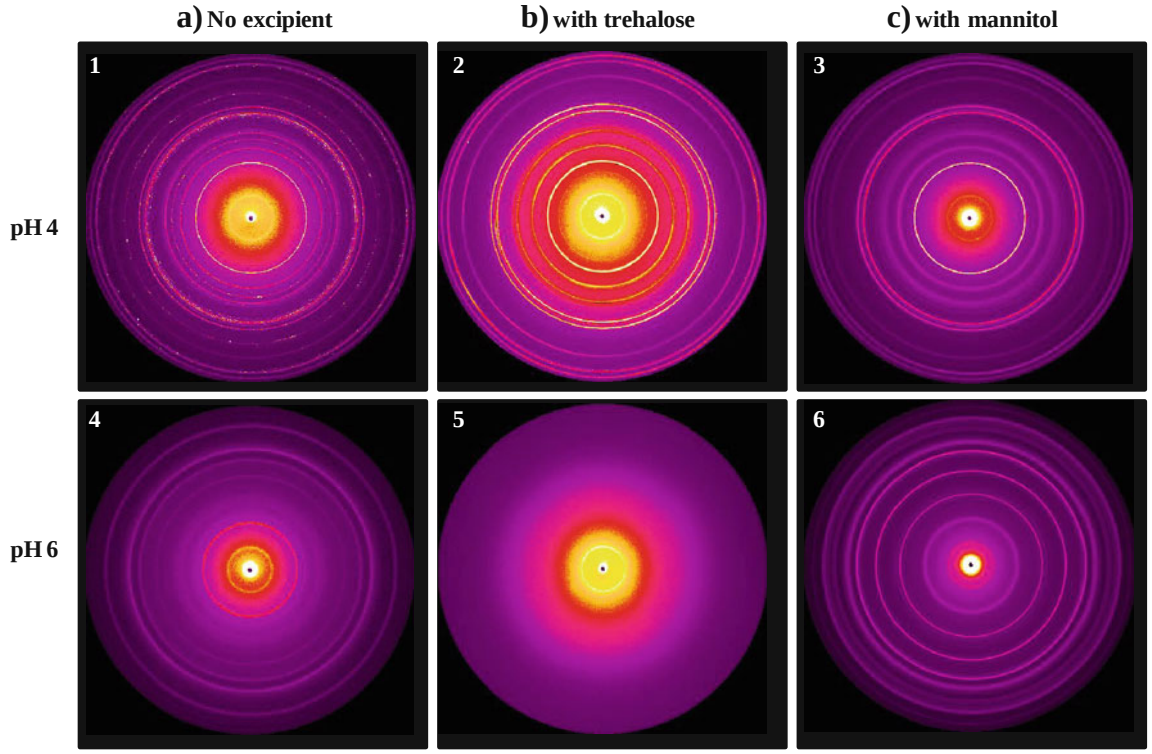

Fig. 1 Two-dimensional synchrotron XRD images of final lyophiles **a** prepared from 10 mM succinic acid buffered to pH values of 4.0 and 6.0, **b** the above solution contain trehalose (2% w/v), **c** buffer solution contain mannitol (2% w/v). The enlarged panel 2 is shown in Fig. 2. As the diameter of the Debye ring increases, there is a decrease in d-spacing (as is evident from Fig. 2).

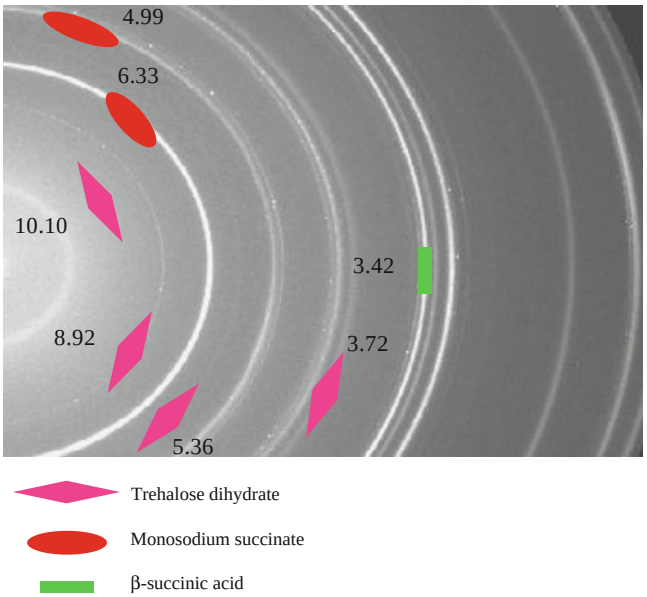

Fig. 2 Two-dimensional synchrotron XRD images of final lyophiles prepared from succinic acid buffer (10 mM; pH 4.0) solution containing 2% w/v trehalose. This is the enlarged panel 2 from Fig. 1.

Characterization of the Frozen Solution

Low Temperature pH Measurement

We had reported that sequential crystallization of succinate buffer components caused a 'pH swing' in the frozen solution (26). Interestingly, this effect depended on the initial buffer concentration. Figure 4 contains the temperature and pH measurements of succinate buffer solution during cooling and annealing. At low buffer concentration

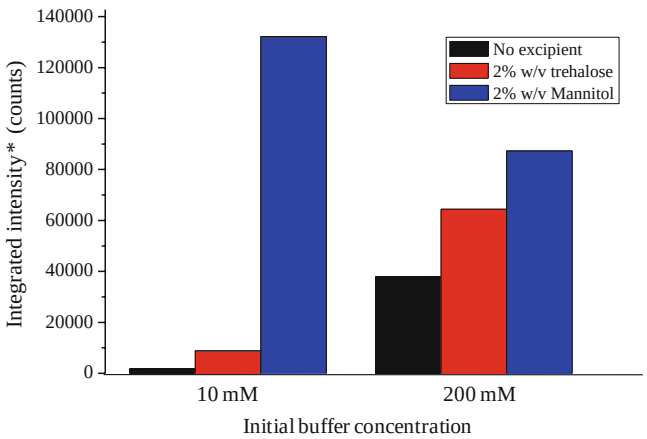

Fig. 3 Histogram displaying the effect of trehalose and mannitol on the integrated intensities of the characteristic peaks of monosodium succinate in the final lyophiles. The succinate buffer concentrations in the prelyophilization solution were 10 and 200 mM with an initial pH value of 4.0. *Sum of the integrated intensities of the 14.0 and 17.8° 2θ peaks of monosodium succinate.

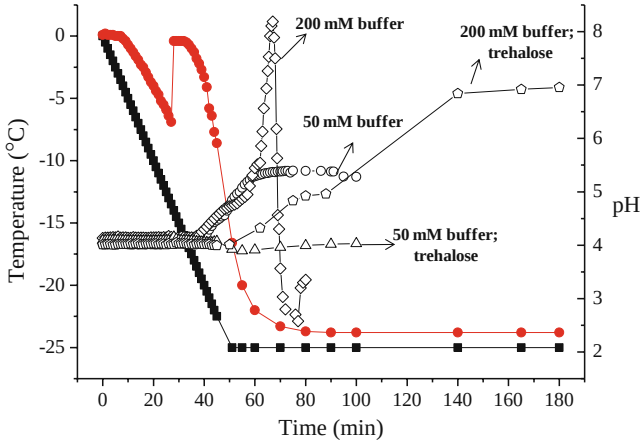

Fig. 4 Low temperature pH of the solutions (initial pH value of 4.0) containing succinate buffer and trehalose (2% w/v) as a function of time. The bath (-■-) and sample (-●-) temperatures were also measured simultaneously.

(50 mM), after an initial lag, the sample temperature decreased at about the same rate as the bath until ice crystallization occurred at ~−8°C. The sample temperature then increased sharply due to the release of latent heat of crystallization. After a substantial fraction of the ice had crystallized, the sample temperature again started to decrease. By this time, the bath temperature had reached −25°C, and annealing had been initiated. The pH of the freeze-concentrate increased to ~5.5 as the solution was annealed due to the crystallization of succinic acid followed by monosodium succinate. However, at the higher buffer concentration (200 mM), the pH initially increased to ~8.0, then decreased to 2.2, and finally increased to 4.0. This pH swing was attributed to the sequential crystallization of succinic acid, monosodium and disodium succinate (26).

In the presence of trehalose, at low initial buffer concentration (50 mM), the pH was unaltered both during cooling and annealing. Thus, trehalose inhibited buffer salt crystallization. However, at the higher buffer concentration (200 mM), the pH gradually increased from 4.0 to ~7.0 during annealing, attributed to the crystallization of succinic acid followed by monosodium succinate. While the pH excursions were much less pronounced and took longer in presence of trehalose, at this high buffer concentration, trehalose did not significantly inhibit buffer crystallization.

We speculate that when the solution containing buffer and trehalose was cooled, ice crystallized, resulting in a freeze-concentrate consisting of buffer components, trehalose, and unfrozen water. Upon crystallization of a fraction of the buffer components from the freeze-concentrate, the associated unfrozen water would also crystallize. This would increase the trehalose concentration in the freeze-concentrate, though the effect on buffer salt concentration is unknown. The buffer component crystals (both succinic

acid and monosodium succinate) might not only facilitate further buffer crystallization but also induce trehalose crystallization, particularly if there is high degree of supersaturation of these solutes.

Low Temperature XRD

In an effort to evaluate the crystallization propensity of trehalose in frozen solutions, a prelyo solution containing trehalose alone was studied. To facilitate solute crystallization, experiments were also performed by seeding the frozen solution with the crystals of either succinic acid or trehalose dihydrate. Figure 5 contains the one-dimensional XRD patterns of frozen trehalose solution, seeded with succinic acid, and recorded as a function of annealing time. The unseeded solution and the system seeded with trehalose dihydrate were discussed earlier (21).

There was no evidence of solute crystallization upon cooling the aqueous trehalose solution to −40°C (not shown). However, the first evidence of trehalose dihydrate crystallization was observed after annealing the frozen solution at −18°C for 12 h. Up to 36 h of annealing, there was a pronounced increase in the intensity of the characteristic peaks indicating that annealing facilitated

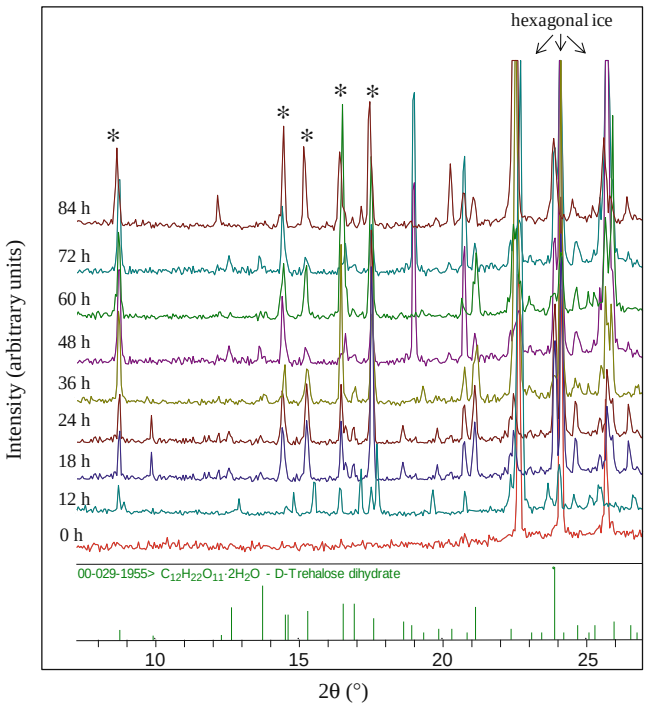

Fig. 5 XRD patterns of frozen aqueous trehalose (4% w/v) solution recorded during annealing. The solution was initially cooled from RT to −40°C, held for 15 min, heated to −18°C and annealed for 84 h. The characteristic peaks of hexagonal ice and trehalose dihydrate (*asterisk*) are pointed out. Prior to annealing, the sample was seeded with crystals of succinic acid. For comparison purposes, the stick pattern of D-trehalose dihydrate obtained from the Powder Diffraction Files of the International Centre for Diffraction Data is provided (29).

further solute crystallization. Based on literature reports and the thermal events observed in trehalose-water binary system (the DSC results are discussed in the next section), the system was annealed at −18°C (16,19,20). Upon annealing the unseeded frozen solution, crystallization of trehalose dihydrate was evident, but only after 3 days (data not shown, see earlier publication) (21). As indicated earlier, seeding either with succinic acid or trehalose dihydrate caused crystallization which could be detected after only 12 h of annealing. As a control, when pure ice seeded either with succinic acid or trehalose dihydrate was subjected to XRD, only the peaks of hexagonal ice were observed.

Experiments were also carried in the synchrotron beamline (in the transmission mode), wherein crystallization of trehalose dihydrate was evident in the seeded (surface sprinkling) system. The details of the experimental setup were provided earlier (21,26). In this custom-designed setup, the sample chamber could be moved along the z-axis, enabling us to monitor trehalose crystallization as a function of depth (Fig. 6). While only hexagonal ice was seen when the solution was cooled (panel a), seeding followed by annealing for 12 h revealed the crystallization of trehalose dihydrate. There was no pronounced difference in the intensity of the trehalose dihydrate peaks as a function of the sample depth, suggesting approximately uniform crystallization of trehalose throughout the frozen mass.

Freezing and Thawing—Characterization by DSC and XRD

Figure 7 contains a representative DSC heating curve of annealed frozen trehalose solution. The unannealed solution served as a control. In an effort to interpret the thermal events observed in the DSC, experiments under similar conditions were carried out in the XRD (Fig. 8). While the heating and cooling rate in the DSC was 1°C/min, in light of the higher sample volume, the cooling and heating rate in the XRD was 0.5°C/min.

XRD revealed only hexagonal ice when the trehalose solution was cooled from RT to −40°C. DSC cooling curve indicated ice crystallization at ~−8°C (not shown). When the frozen solution was seeded and warmed back to RT without annealing, first a glass transition event was observed at ~−32°C, followed by ice melting at ~−0.8°C (Fig. 7, bottom curve). However, when the sample was warmed to RT after annealing for 48 h, an endotherm attributable to eutectic melting event was observed at −2.8°C (Fig. 7, top curve) followed by ice melting. A similar experiment was conducted in the XRD sample chamber (Fig. 8). After the sample was cooled to −40°C, seeded, and annealed for 48 h, crystallization of trehalose dihydrate was evident (not shown). XRD patterns were continuously collected as the sample was

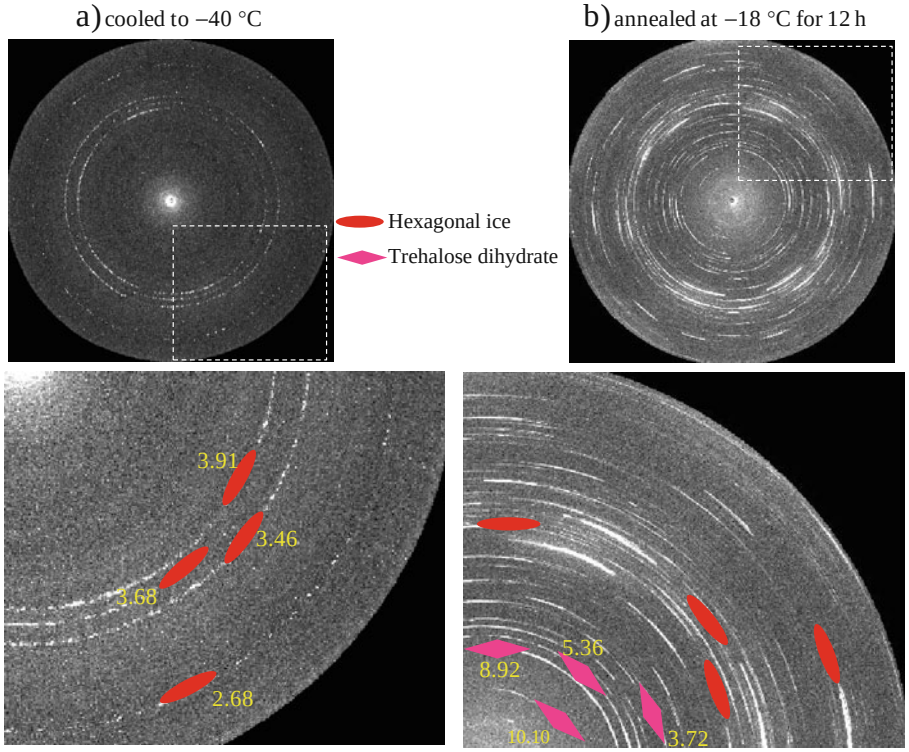

Fig. 6 Two-dimensional synchrotron XRD image of frozen aqueous trehalose solution recorded **a** soon after cooling to −40°C and **b** after annealing at −18°C for 12 h. Prior to annealing, the frozen sample (panel 1) was seeded with succinic acid crystals. Both the cooling and heating rates were 1°C/min. The enlarged view of the XRD image shows some characteristic Debye rings (in Å units) of hexagonal ice and trehalose dihydrate.

warmed to RT (Fig. 8, top to bottom patterns increasing temperature). The characteristic peaks of trehalose dihydrate were observed even in the scan collected at −3°C. This is contrary to the earlier reported eutectic temperatures (−18.8 and −4.4°C) of the trehalose-water system. However, the trehalose dihydrate peaks disappeared completely when the temperature was increased to −2°C. This indicated that the eutectic temperature of trehalose dihydrate-ice was between −2 and −3°C. Eventually, ice peaks also disappeared at −1°C. Thus, XRD provided direct evidence of eutectic melting and complemented the DSC results. The eutectic temperatures, obtained by DSC and XRD, were in close agreement with that reported by Miller *et al.* (18).

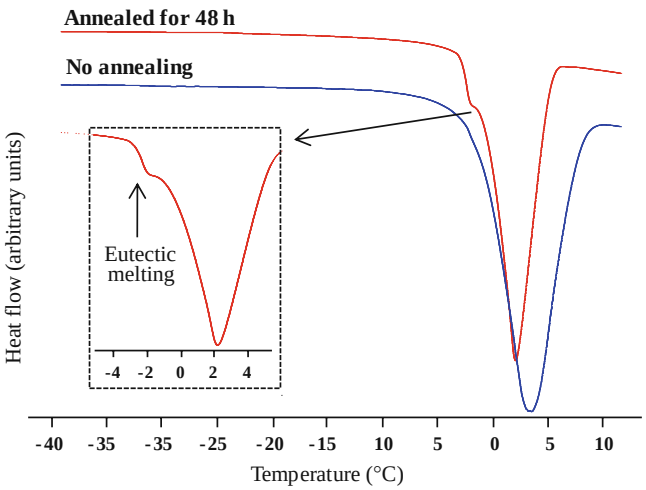

Fig. 7 DSC heating curves of frozen aqueous trehalose (4% w/v) solutions. The solutions were cooled from RT to −70°C, held for 15 min, and either (i) warmed to RT without annealing or (ii) warmed to −18°C and annealed for 48 h and then cooled back to −50°C and rewarmed to RT. Both the heating and cooling rates were 1°C/min. The eutectic melting temperature is pointed out in the inset.

Phase Transformation during Freeze-Drying

While both XRD (Figs. 5 & 6) and DSC (Fig. 7) provided unequivocal evidence of annealing-induced trehalose crystallization in the frozen solution, there are numerous reports documenting amorphous trehalose in the final lyophile (2,9–11,13–16,18–20). This conclusion is often based on the physical characterization of the dried product. This raises the interesting question: Can the trehalose dihydrate, which crystallized in the frozen solution, undergo a crystalline dihydrate → amorphous anhydrate transition during drying? Such a phase transformation has been observed in numerous organic and inorganic hydrates (8,21,27). The kinetics of water removal, governed by the dehydration temperature and water vapor pressure, can dictate the physical state of the dried solid. In addition to the two extremes in lattice

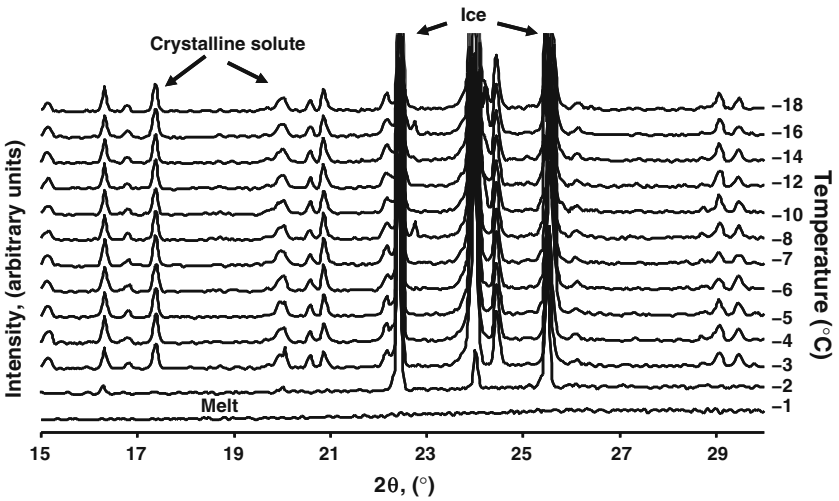

Fig. 8 XRD patterns of the binary system containing trehalose dihydrate and ice recorded during warming. The sample was initially cooled to −50°C, held for 15 min, warmed to −18°C, seeded with trehalose dihydrate and annealed for 48 h. Some of the characteristic peaks of trehalose dihydrate and ice are pointed out.

order (crystalline and amorphous), partially crystalline product phase may also be obtained.

During drying, dehydration of hydrate, such as disodium phosphate dodecahydrate (31) and raffinose pentahydrate, (8) yielded the respective amorphous anhydrous phases. Recently, we reported the transformation of disodium succinate hexahydrate to amorphous anhydrate during drying (21). In an effort to monitor phase transitions during freeze-drying of trehalose solution, the entire freeze-drying cycle was carried out in the sample chamber of the X-ray diffractometer. The XRD patterns collected during primary and secondary drying are shown in Fig. 9.

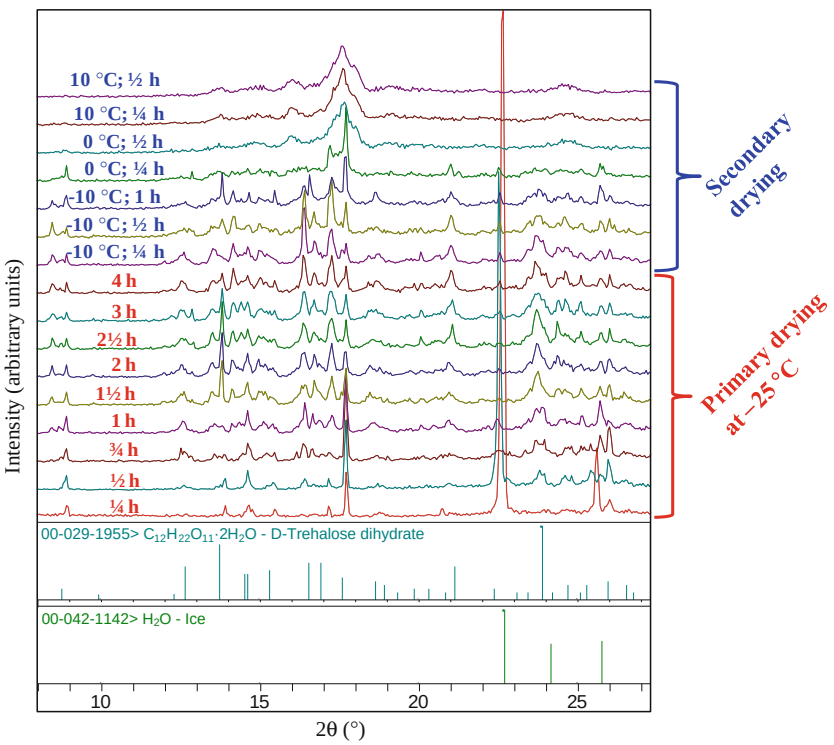

Fig. 9 XRD patterns of frozen aqueous trehalose solution recorded during the drying stages of lyophilization. The sample was initially cooled from RT to −40°C, held for 15 min, warmed to −18°C, seeded with succinic acid, and annealed for 94 h. The cooling and heating rate was 1°C/min. For comparison purposes, the stick patterns of hexagonal ice and D-trehalose dihydrate obtained from the Powder Diffraction Files of the International Centre for Diffraction Data are provided.

The XRD pattern obtained soon after cooling to −40°C revealed ice crystallization (data not shown). Annealing at −18°C resulted in the crystallization of trehalose dihydrate. There was a progressive increase in the intensity of the trehalose dihydrate peaks as a function of annealing time (data not shown). After 84 h of annealing, the primary drying was performed at −25°C and then the secondary drying was carried out, first at −10 and then at 0 and 10°C (Fig. 9).

During primary drying at −25°C, ice sublimation was evident from the gradual decrease in intensity of ice peaks, which disappeared completely after 30 min of drying. This was followed by a gradual and pronounced decrease in the intensity of trehalose dihydrate peaks, indicating dehydration. The dehydration process did not result in the appearance of new peaks. Instead, an amorphous halo appeared over the angular range of 12 to 18° 2θ. Dehydration was not complete even after 3 h of primary drying. However, when the secondary drying was initiated by raising the temperature to −10°C, there was a pronounced decrease in the intensity of trehalose dihydrate peaks. When the secondary drying temperature was progressively increased, first to 0 and then to 10°C, trehalose dihydrate peak intensities progressively decreased, and the peaks eventually disappeared. Interestingly, after drying for about 30 min at 0 C, the most intense peak at 17.8° 2θ, of the anhydrous α-trehalose appeared. The broad peaks, observed over the angular range of 12 to 18° 2θ, reflected the existence of short-range order in the final dried product. The continued existence of α-trehalose is evident from the peak at 17.8° 2θ.

SIGNIFICANCE

The hydrogen bonding between the hydroxyl groups of amorphous sugars and the polar residues in proteins is one possible mechanism of protein stabilization by sugars in the dry state (25). Lyoprotectant phase separation, whether or not followed by crystallization, can result in protein-rich and lyoprotectant-rich domains (5). Once phase separation is brought about by trehalose crystallization in the frozen solution, it is no longer available to stabilize the protein. While trehalose may undergo a crystalline hydrate → amorphous anhydrate transition during drying, it continues to remain phase separated. Therefore, its ability to stabilize the protein may be seriously compromised.

The widespread use of trehalose is a testament to its effectiveness as a lyoprotectant. However, this work reveals its propensity to undergo annealing-induced crystallization and then transform to an amorphous anhydrate during drying. Thus, in the absence of annealing or seeding, trehalose may not crystallize at all in the frozen system. It is also possible, and quite likely, that only a fraction of the trehalose crystallized. The uncrystallized or the amorphous fraction may be an effective lyoprotectant. However, once trehalose crystallization is initiated, the crystals may act as seeds and promote further crystallization during storage. While this process may be very slow, it may occur to a significant extent in the timescales of product storage. Hence, there is a potential, not only for product failure but also for batch-to-batch variation in product performance.

The current investigation focused on the crystallization behavior of trehalose in the absence of cosolute. The presence of noncrystallizing cosolutes, particularly macromolecules, may effectively inhibit trehalose crystallization. On the other hand, as was observed in the presence of succinic acid, crystallizing cosolutes may facilitate trehalose crystallization (32). Several other commonly used formulation components, including mannitol, glycine and sodium chloride, crystallize readily. It was therefore of interest to evaluate the effect of readily crystallizing cosolutes as well as noncrystallizing model APIs on trehalose crystallization. This is the subject of our next manuscript (32).

CONCLUSIONS

In frozen solutions, both DSC and XRD revealed annealing-induced crystallization of trehalose dihydrate. However, during drying, dehydration of trehalose dihydrate yielded a substantially amorphous lyophile. Therefore, analysis of the final lyophile may not reveal trehalose crystallization during freeze-drying. In such cases, it is imperative that the system is monitored during all the stages of freeze-drying. The phase separation of trehalose can have serious implications on protein stability.

REFERENCES

1. Pikal MJ. Freeze drying. In: Swarbrick J, editor. Encyclopedia of pharmaceutical technology, vol. 1. New York: Informa healthcare; 2007. p. 1807–33.
2. Anhorn MG, Mahler H-C, Langer K. Freeze drying of human serum albumin (HSA) nanoparticles with different excipients. Int J Pharm. 2008;363:162–9.
3. Imamura K, Asano Y, Maruyama Y, Yokoyama T, Nomura M, Ogawa S, *et al.* Characteristics of hydrogen bond formation between sugar and polymer in freeze-dried mixtures under different rehumidification conditions and its impact on the glass transition temperature. J Pharm Sci. 2008;97:1301–12.
4. Izutsu K, Yoshioka S, Takeda Y. The effects of additives on the stability of freeze-dried beta -galactosidase stored at elevated temperature. Int J Pharm. 1991;71:137–46.
5. Izutsu K, Yoshioka S, Terao T. Decreased protein-stabilizing effects of cryoprotectants due to crystallization. Pharm Res. 1993;10:1232–7.
6. Randolph TW. Phase separation of excipients during lyophilization: effects on protein stability. J Pharm Sci. 1997;86:1198–203.

7. Carpenter JF, Pikal MJ, Chang BS, Randolph TW. Rational design of stable lyophilized protein formulations: some practical advice. Pharm Res. 1997;14:969–75.
8. Chatterjee K, Shalaev EY, Suryanarayanan R. Raffinose crystallization during freeze-drying and its impact on recovery of protein activity. Pharm Res. 2005;22:303–9.
9. Coutinho C, Bernardes E, Felix D, Panek AD. Trehalose as cryoprotectant for preservation of yeast strains. J Biotechnol. 1988;7:23–32.
10. Crowe JH, Carpenter JF, Crowe LM. The role of vitrification in anhydrobiosis. Annu Rev Physiol. 1998;60:73–103.
11. Crowe LM, Reid DS, Crowe JH. Is trehalose special for preserving dry biomaterials? Biophys J. 1996;71:2087–93.
12. Lu X, Pikal MJ. Freeze-drying of mannitol-trehalose-sodium chloride-based formulations: The impact of annealing on dry layer resistance to mass transfer and cake structure. Pharm Dev Technol. 2004;9:85–95.
13. Akers MJ. Excipient—drug interactions in parenteral formulations. J Pharm Sci. 2002;91:2283–300.
14. Surana R, Pyne A, Suryanarayanan R. Effect of aging on the physical properties of amorphous trehalose. Pharm Res. 2004;21:867–74.
15. Surana R, Pyne A, Suryanarayanan R. Effect of preparation method on physical properties of amorphous trehalose. Pharm Res. 2004;21:1167–76.
16. Miller DP, De Pablo JJ. Calorimetric solution properties of simple saccharides and their significance for the stabilization of biological structure and function. J Phys Chem B. 2000;104:8876–83.
17. Bubnik Z, Kadlec P. Sucrose solubility. In: Mathlouthi M, Reiser P, editors. Sucrose properties and applications. Glasgow: Blackie Academic & Processional; 1995. p. 101–25.
18. Miller DP, De Pablo JJ, Corti H. Thermophysical properties of trehalose and its concentrated aqueous solutions. Pharm Res. 1997;14:578–90.
19. Green JL, Angell CA. Phase relations and vitrification in saccharide-water solutions and the trehalose anomaly. J Phys Chem. 1989;93:2880–2.
20. Nicolajsen H, Hvidt A. Phase behavior of the system trehalose-NaCl-water. Cryobiology. 1994;31:199–205.
21. Sundaramurthi P, Suryanarayanan R. Trehalose crystallization during freeze-drying: Implications on lyoprotection. J Phys Chem Lett. 2010;1:510–4.
22. Akers MJ, Vasudevan V, Stickelmeyer M. Formulation development of protein dosage forms. Pharm Biotechnol. 2002;14:47–127.
23. Han J, Suryanarayanan R. Influence of environmental conditions on the kinetics and mechanism of dehydration of carbamazepine dihydrate. Pharm Dev Technol. 1998;3:587–96.
24. Han J, Suryanarayanan R. A method for the rapid evaluation of the physical stability of pharmaceutical hydrates. Thermochim Acta. 1999;329:163–70.
25. Allison SD, Chang B, Randolph TW, Carpenter JF. Hydrogen bonding between sugar and protein is responsible for inhibition of dehydration-induced protein unfolding. Arch Biochem Biophys. 1999;365:289–98.
26. Sundaramurthi P, Shalaev E, Suryanarayanan R. "pH swing" in frozen solutions-consequence of sequential crystallization of buffer components. J Phys Chem Lett. 2010;1:265–8.
27. Sundaramurthi P, Shalaev E, Suryanarayanan R. Calorimetric and diffractometric evidence for the sequential crystallization of buffer components and consequent pH swing in frozen solutions. J Phys Chem B. 2010;114:4915–23.
28. Moore TW. Dissolution testing: a fast, efficient procedure for degassing dissolution medium. Dissolution Technol. 1996;3:3–5.
29. Powder Diffraction File. Hexagonal ice, card # 00-042-1142; D-trehalose dihydrate, card # 00-029-1955; trehalose anhydrate, card # 00-003-0312. *International Centre for Diffraction Data, Newtown Square, PA* (2004).
30. Varshney DB, Kumar S, Shalaev EY, Sundaramurthi P, Kang S-W, Gatlin LA, *et al.* Glycine crystallization in frozen and freeze-dried systems: effect of pH pH and buffer concentration. Pharm Res. 2007;24:593–604.
31. Pyne A, Chatterjee K, Suryanarayanan R. Crystalline to amorphous transition of disodium hydrogen phosphate during primary drying. Pharm Res. 2003;20:802–3.
32. Sundaramurthi P, Suryanarayanan R. Influence of crystallizing and non-crystallizing cosolutes on trehalose crystallization during freeze-drying. Pharm Res. 2010; doi:10.1007/s11095-010-0221-8.